Direct synthesis design of Cu-SAPO-18, a very efficient catalyst for the SCR of NOx

Raquel Martínez-Franco, Manuel Moliner*, Avelino Corma*

Instituto de Tecnología Química (UPV-CSIC), Universidad Politécnica de Valencia, Consejo Superior de Investigaciones Científicas, Valencia, 46022, Spain

*Corresponding authors: E-mail addresses: acorma@itq.upv.es; mmoliner@itq.upv.es

Abstract

The combination of Cu(II) triethylenetetramine and N,N-dimethyl-3,5-dimethylpiperidinium as structure directing agents allowed the direct preparation of highly active and hydrothermally stable Cu-SAPO-18 active for the selective catalytic reduction of NOx with NH_3. The approach allows performing a one-pot synthesis avoiding intermediate calcination and ion exchange, while achieving complete framework Si isolation. Combination of physicochemical characterization techniques show that copper exists as extra-framework Cu^{2+}, which have been identified as the specific active sites for the SCR of NOx. The selective presence of isolated Si species in the zeolitic framework introduces high hydrothermal stability.

Graphical abstract
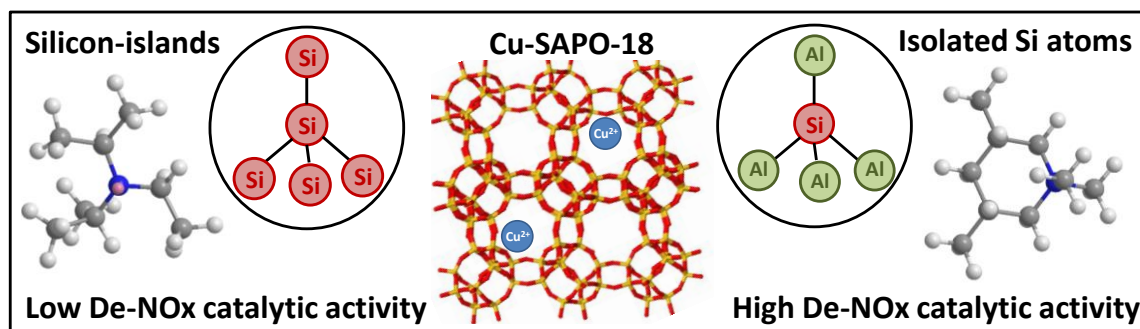
Highlights

- Specific cyclic ammonium cations allow the direct synthesis of Cu-SAPO-18 catalysts.
- Complete framework Si isolation can be achieved for Cu-SAPO-18 materials.
- Cu-SAPO-18 shows high catalytic activity and hydrothermal stability for SCR of NOx.

1.- Introduction

In the last decades, small pore zeolites containing large cavities in their structure have become important industrial catalysts for the methanol-to-olefins (MTO) process, and for the field of gas separation.[1] In addition, these materials have recently broadened their applicability as efficient catalysts to control the emission of harmful gases, particularly nitrogen oxides (NOx) mainly produced during the high temperature combustion in diesel engines.[1,2] Indeed, the selective catalytic reduction (SCR) of NOx by ammonia or urea has been reported as the most widely applied emission control,[3] and copper-exchanged small pore CHA materials as one of the preferred catalysts (either as silicoaluminate, Cu-SSZ-13,[1,2,4] or as silicoaluminophosphate, Cu-SAPO-34).[2,5]

Small pore Cu-CHA shows higher catalytic activities and hydrothermal stabilities for the SCR of NOx than other previously studied zeolites with larger pores (as Cu-Beta or Cu-ZSM-5, among others).[6] This is a very important point because the SCR of NOx reaction is performed in the presence of steam at high temperatures (above 400ºC) and, under these severe conditions, Cu-Beta or Cu-ZSM-5 zeolites suffer from permanent deactivation.[6] Specific stabilization issues by coordination of extra-framework Cu^{2+} cations to three oxygen atoms of the double 6-rings (D6R) units present in the CHA structure have been described as the main reason of the improved catalytic activity and hydrothermal stability of the Cu-CHA catalysts.[7]

Besides Cu-exchanged CHA, other Cu-exchanged small pore silicoaluminates containing D6R in their structure have been reported as efficient catalyst for the SCR of NOx, as Cu-SSZ-16 [8] and Cu-SSZ-39.[9] Particularly, Cu-SSZ-39, which presents the AEI structure, shows very high catalytic activity and hydrothermal stability for the SCR of NOx, even higher than commercial Cu-SSZ-13 catalyst.[9] Unfortunately, the range of preparation conditions of the silicoaluminate SSZ-39 is very limited, requiring very narrow Si/Al synthesis ratios (~30) and specific chemical sources, as for instance partially dealuminated USY and sodium silicate as Al and Si sources, respectively.[10] Moreover, the relatively low Si/Al ratios of the final SSZ-39 materials (~7-10) compared to the synthesis Si/Al ratios,

indicate that the solid yields are low (< 50%wt of initial oxides),[9,10] and this fact precludes possible industrial applications.

The AEI structure has also been reported as silicoaluminophosphate form, SAPO-18,[11] which is mainly synthesized using N,N-diisopropylethylamine (DIPEA) as organic structure directing agent (OSDA).[11,12] SAPO-18 has been thoroughly used as catalyst for the MTO reaction,[13] but very few descriptions can be found in the literature for the SCR of NOx using Cu-exchanged SAPO-18.[14] Indeed, these Cu-exchanged SAPO-18 materials show moderate SCR-DeNOx catalytic activities and low hydrothermal stabilities, probably as a result of the large presence of Si-rich domains as Si-islands. In fact, the formation of these Si-rich domains take place by multiple substitutions of Al^{3+} and P^{5+} with Si^{4+} atoms in tetrahedral coordination, resulting in neutral silicon domains that very weakly stabilize the extra-framework cationic species.[15, 16] In contrast, if a selective isomorphic substitution of P^{5+} with isolated Si^{4+} atoms in tetrahedral framework positions may take place, an improved stabilization of the extra-framework cationic species and, consequently, of the overall catalyst may occur by the selective introduction of negative charges in the zeolitic framework.[11]

Very recently, different direct syntheses of Cu-containing small pore zeolites, especially CHA polymorphs, have been reported in the literature using inexpensive cationic organometallic complexes.[5b, 5c, 16, 17] These "one-pot" syntheses procedures are very interesting because the multiple steps required in the conventional post-synthetic metal ion-exchange methodologies (zeolite synthesis, calcination, cationic exchange, and calcination) are avoided. The direct synthesis of metal-containing zeotypes not only allows optimizing the preparation of these materials in terms of reducing the number of synthesis steps, but also improving their physico-chemical properties.[16] For the particular case of Cu-SAPO-34, the hydrothermal stability of this catalyst has been considerably increased by properly modifying the synthesis conditions to favor the selective distribution of isolated Si species in the framework positions by direct synthesis methodologies.[16]

Herein, we propose for the first time the direct synthesis of Cu-SAPO-18 to obtain a highly active and hydrothermally stable catalyst for the SCR of NOx. To do this, a rationalized use of cooperative OSDAs is proposed, consisting in the combination of an organometallic Cu-complex (Cu^{2+} with tetraethylenepentamine [TEPA] or triethylenetetramine [TETA]) with another organic molecule able to direct the crystallization towards the SAPO-18. The use of the N,N-dimethyl-3,5-dimethylpiperidinium (DMDMP) as co-template is shown for the first time to synthesize any aluminophosphate-related form of SAPO-18. Very interestingly, the direct synthesis of Cu-SAPO-18 materials by combining a Cu-polyamine complex and DMDMP as co-OSDA allows the crystallization of catalysts with high solid yields, isolated Si species in the zeolitic framework, controlled amount of extra-framework cationic species of copper in the final solids, and excellent catalytic activities and hydrothermal stabilities for the SCR of NOx.

2.- Experimental

2.1.- <u>Synthesis</u>

2.1.1.- <u>N,N-dimethyl-3,5-dimethylpiperidinium (DMDMP) synthesis</u>

10 g of 3,5-dimethylpiperidine (Sigma-Aldrich, ≥ 96 %wt) and 19.51 g of potassium bicarbonate ($KHCO_3$, Sigma-Aldrich; 99.7%wt) were dissolved in 140 ml of methanol. Later, 54 ml of methyl iodide (CH_3I, Sigma-Aldrich, ≥ 99%wt) was added dropwise, and the mixture stirred at room temperature for 5 days. After this period, the mixture was filtered to remove most of the potassium bicarbonate, and the solution washed several times with chloroform. The combined organic extracts were dried over $MgSO_4$, filtered and finally, the quaternary ammonium salt (85 % yield) was precipitated with diethyl ether. The iodide salt was converted to the hydroxide salt by treatment with a hydroxide anion exchange resin (Dower SBR).

2.1.2.- <u>Direct synthesis of Cu-SAPO-18 materials</u>

In a general procedure for the Cu-SAPO-18 preparation, the Cu-complex was first prepared by mixing a 20%wt of an aqueous solution of copper (II) sulfate (98%wt, Alfa)

with the required amount of triethylenetetramine (TETA, 99%wt, Aldrich) or tetraethylenepentamine (TEPA, 98%wt, Aldrich). This mixture was stirred for 2 hours until complete dissolution. Second, distilled water and phosphoric acid (85% wt, Aldrich) were added to the above solution and stirred for 5 minutes. Third, the co-OSDA organic molecule, either N,N-diisopropylethylamine (DIPEA, 99%wt, Aldrich) or N,N-dimethyl-3,5-dimethylpiperidinium (DMDMP) was introduced in the gel mixture. Finally, alumina (75%wt, Condea) and silica (Ludox AS40 40%wt, Aldrich) sources, were added in the gel, and the mixture was stirred for 30 minutes. The resulting gel was transferred to an autoclave with a Teflon liner, and heated at the desired temperature under dynamic conditions for the required time. Crystalline products were filtered and washed with abundant water, and dried at 100ºC overnight. The samples were calcined at 550ºC in air to properly remove the occluded organic species.

2.1.3.- Cu-exchanged SAPO-18

SAPO-18 was synthetized according to the procedure described in reference [11], using DIPEA as OSDA and the following molar gel composition: 1 Al_2O_3: 0.85 P_2O_5: 0.3 SiO_2: 1.85 OSDA: 18.5 H_2O. The crystalline sample was calcined at 550 ºC in air to remove the occluded organic species. The calcined sample was washed with $NaNO_3$ (0.04 M), and afterwards, cation exchanged overnight at room temperature with a $Cu(CH_3CO_2)_2$ solution (solid/liquid ratio of 100 g/l). The sample was filtered and washed with abundant distilled water, and finally, calcined at 550 ºC for 2 h.

2.2.- Characterization

Powder X-ray diffraction (PXRD) measurements were performed with a multisample Philips X'Pert diffractometer equipped with a graphite monochromator, operating at 40 kV and 45 mA, and usig Cu K_α radiation (λ = 0,1542 nm).

The chemical analyses were carried out in a Varian 715-ES ICP-Optical Emission spectrometer, after solid dissolution in HNO_3/HCl/HF aqueous solution. The organic content of as-made materials was determined by elemental analysis performed on a SCHN FISONS element analyzer.

The morphology of the samples was studied by scanning electron microscopy (SEM) using a JEOL JSM-6300 microscope and by field emission scanning electron microscopy (FESEM) using a ZEISS Ultra-55 microscope.

The ^{29}Si MAS NMR spectra were recorded at room temperature with a Bruker AV 400 spectrometer MAS, with a spinning rate of 5 kHz at 79.459 MHz with a 55° pulse length of 3.5 μs and repetition time of 180 s. ^{29}Si chemical shift was referred to tetramethylsilane.

UV–Vis spectra were obtained with a Perkin–Elmer (Lambda 19) spectrometer equipped with an integrating sphere with $BaSO_4$ as reference.

Temperature-programmed reduction (TPR) experiments were carried out in a Micromeritics Autochem 2910 equipment.

2.3.- Catalytic experiments

The catalytic activity of the samples for the selective catalytic reduction of NOx using NH_3 as reductor was tested in a fixed bed, quartz tubular reactor of 1.2 cm of diameter and 20 cm of length. The total gas flow was fixed at 300 ml/min, containing 500 ppm of NO, 530 ppm of NH_3, 7% of O_2, and 5% of H_2O. The catalyst (40 mg) was introduced in the reactor, heated up to 550ºC and maintained at this temperature for one hour under nitrogen flow. Then, the desired reaction temperature was set (170-550ºC) and the reaction feed admitted. The NOx present in the outlet gases from the reactor was analyzed continuously by means of a chemiluminiscence detector (Thermo 62C).

2.4.- Steaming procedure

The hydrothermal stability of metal-containing molecular sieves was studied by steaming with water (2.2 mL/min) at 750ºC for 13 hours.

3.- Results and discussion

3.1.- Direct synthesis of Cu-SAPO-18: Diisopropylethylamine as OSDA

The preferred synthesis of the silicoaluminophosphate SAPO-18 in the literature uses N,N-diisopropylethylamine (DIPEA) as OSDA.[11,12] Based on our previous reports for the direct

synthesis of Cu-containing SAPO-34 materials,[5b,16] we propose the one-pot synthesis of the Cu-SAPO-18 material by combining N,N-diisopropylethylamine as OSDA with an organometallic Cu-complex, such as Cu-triethylenetetramine (Cu-TETA) or Cu-tetraethylenepentamine (Cu-TEPA). Different synthesis variables will be studied, including two silicon contents [Si/(Al+P)=0.053, 0.081], two Cu-complexes (Cu-TETA and Cu-TEPA), and two Cu-complex ratios [Cu-complex/(Al+P) = 0.025, 0.05].

As shown in Figure 1, crystalline Cu-SAPO-18 materials can be achieved using both Cu-TETA and Cu-TEPA complexes, preferentially when the Cu-complex content introduced in the synthesis gel is low [Cu-complex/(Al+P)=0.025]. However, the crystallization of Cu-SAPO-18 with higher Cu-contents in the synthesis gel is only favored using Cu-TETA as Cu-complex (see CuSAPO18_4 in Figure 1), obtaining Cu-SAPO-34 when using Cu-TEPA. This fact could be explained by the preferential directing effects of the Cu-TEPA complex towards the CHA cavity present in SAPO-34, as it has been previously described.[17a]

The PXRD patterns reveal the absence of impurities and the high crystalline nature of the as-synthesized Cu-SAPO-18 materials (see Figure 2). To validate the incorporation of the Cu atoms and their extra-framework cationic nature, CuSAPO18_1 has been characterized. On one hand, ICP analyses indicate that 2.6%wt of Cu has been incorporated (see Table 1) and, most interestingly, the UV-Vis spectrum of the as-prepared CuSAPO18_1 shows the presence of the Cu-TEPA complex molecules intact in the final solid, as reveals the single band centered at ~260 nm, which is essentially the same to the observed in the UV-Vis spectrum of the Cu-TEPA complex in solution (see Figure 3). This is an important point because extra-framework Cu^{2+} species will be preferentially formed after calcination, which have been described as the selective active sites for the SCR of NOx reaction.[4b]

^{29}Si MAS NMR spectroscopy has been used to study the coordination of the silicon in the CuSAPO18_1 catalyst. As shown in Figure 4, a very broad signal centered at -110 ppm is mainly observed for the CuSAPO18_1 catalyst. This signal has been assigned to Si rich environments forming "silicon islands" and, unfortunately, these silicon domains will not be able to efficiently stabilize the presence of extra-framework cations, which will mainly

be stabilized by structural defects. It is important to note that similar silicon distributions have been reported in the literature for most of the silicoaluminosfosfate SAPO-18 materials.[11,12]

Since the catalytic extra-framework metallic active sites would be weakly stabilized by structural defects, it is expected that this poor metal stabilization may result in catalysts with low activities and hydrothermal stabilities for the SCR of NOx. Indeed, the four crystalline Cu-SAPO-18 materials synthesized using N,N-diisopropylethylamine as OSDA have been tested for the SCR of NOx and, as expected, all of them show low to medium catalytic activity, achieving only acceptable NO conversion values (~ 80%) at reaction temperatures above 450ºC (see Figure 5).

3.2.- Direct synthesis of Cu-SAPO-18: Cyclic ammonium cations as OSDA

- Synthesis and characterization

It is clear that to increase the catalytic activity and hydrothermal stability for the SCR of NOx of small pore SAPOs, the silicon distribution of the Cu-SAPO-18 materials must be improved. However, the synthesis of the SAPO-18 in the literature has been limited, up to now, to the use of N,N-diisopropylethylamine or tetraethylammonium as OSDAs and, in both cases, poor silicon distributions with large amount of "silicon islands" have been observed.[11,12] At this point, we propose for the first time the use of cyclic ammonium cations, such as N,N-dimethyl-3,5-dimethylpiperidinium (DMDMP), as OSDAs for the synthesis of SAPO-18. We base this hypothesis on the fact that related organic molecules have been previously used as efficient OSDAs for the synthesis of the silicoaluminate SSZ-39, isostructural to the SAPO-18 zeotype.[10a] Interestingly, these cyclic ammonium cations are very specific for the cavity of the SSZ-39 zeolite,[10b] and thus, their use as OSDAs for the synthesis of the SAPO-18 may favor the silicon distribution within the structure due to its improved guest/host fitting between the OSDA and the zeolite cavity.

Different experiments have been proposed to study the directing effects of the DMDMP as OSDA towards the "one-pot" synthesis of the Cu-SAPO-18. Previous results indicated

that the synthesis of Cu-SAPO-18 materials can be broadened when using Cu-TETA as Cu-complex and a Si/(Al+P) ratio of 0.081 (see CuSAPO18_3 and CuSAPO18_4 in Figure 1). Besides these parameters, the water [H_2O/(Al+P)= 10, 30] and Cu-complex [Cu-TETA/(Al+P) = 0.025, 0.05, 0.1] ratios have also been varied. The crystallization of these materials has been carried out at 175ºC for 6 days under dynamic conditions. As shown in Figure 6, crystalline SAPO-18 materials have been achieved for the three Cu-contents when the gels are highly diluted [H_2O/(Al+P)=30]. The PXRD patterns of these three Cu-SAPO-18 materials reveal good crystallinity and the absence of competing crystalline phases (see Figure 7).

Chemical analyses indicate that the Cu content in the Cu-SAPO-18 samples can be controlled depending on the initial Cu-complex amount in the synthesis gels (see CuSAPO18_5, _6, and _7 in Table 1). The as-prepared Cu-SAPO-18 material synthesized with the intermediate Cu-content, CuSAPO18_6, has been characterized by UV-VIS spectroscopy to study the coordination of the Cu species. As shown in Figure 8, the UV-VIS spectrum of the as-prepared CuSAPO18_6 material shows a main band centered at 265 nm, which can be assigned to the Cu-TETA complex intact in the final solid. Moreover, elemental and chemical analyses of the CuSAPO18_6 material shows a stoichiometric amount of TETA molecules and Cu (see Table 1), clearly confirming the stability of the Cu-TETA complex in the as-prepared CuSAPO18_6.

The silicon distribution of the as-prepared CuSAPO18_6 has been studied by solid ^{29}Si MAS NMR spectroscopy. The ^{29}Si MAS NMR spectrum exhibits a single peak centered at -90 ppm, which corresponds to the exclusive presence of isolated silicon atoms in Si(4Al) coordination (see CuSAPO18_6 in Figure 4). Interestingly, this result validates our hypothesis of using a more specific OSDA towards the AEI cavity in order to improve the Si distribution along the metal-containing SAPO-18.

These three Cu-SAPO-18 materials have also been characterized by scanning electron microscopy, revealing the formation of crystal aggregates with irregular shape and average sizes ranging from 2 to 10 μm (see Figures 9a, b and c for CuSAPO18_5, _6 and _7,

respectively). Nevertheless, the limited quality of the SEM images does not allow illustrating the real morphology of these aggregates. Thus, to obtain improved images of the crystals, the CuSAPO18_6 has been studied by field emission scanning electron microscopy (FE-SEM). This technique allows better image resolutions due to a more intensive and monochromatic electronic beam. As it can be seen in Figure 9d, the sample is formed by the intergrowth of large cubic crystals of ~ 2-5 μm, agglomerated by some bulk fine powder.

- *Catalysis and hydrothermal stability*

The catalytic activity of CuSAPO18_5, _6, _and _7 materials has been evaluated for the SCR of NOx. These Cu-SAPO-18 catalysts synthesized using the specific DMDMP organic molecule towards the AEI cavity, show much higher catalytic activity than the other Cu-SAPO-18 prepared using less specific OSDAs (see Figures 10a and 5, respectively). Indeed, the catalysts synthesized using DMDMP as OSDA allow NO conversion values above 80%, regardless the Cu content, under broad reaction temperatures (250-500ºC). It is worth mentioning that the sample with the intermediate Cu content, CuSAPO18_6, shows the best catalytic behavior reporting NO conversions of almost 100% (see Figure 10a). This result indicates that an optimized Cu content in the Cu-SAPO-18 catalysts maximizes the catalytic activity for the SCR of NOx under the studied reaction conditions. Recently, we have described similar optimized intermediate Cu-contents for CHA-related structures, such as SAPO-34 [5b,16] and SSZ-13,[17b] to maximize the De-NOx catalytic activity and, most importantly, to maximize the hydrothermal stability of the catalyst.

Very interestingly, these fresh Cu-SAPO-18 catalysts, especially CuSAPO18_6, perform similarly to industrially relevant Cu-SAPO-34 catalysts that have been recently described in the literature.[16, 18] These results points out the relevance that the new Cu-containing SAPO-18 catalysts may have in the current De-NOx scenario if they show high hydrothermal stability after being treated under severe ageing conditions.

A Cu-exchanged SAPO-18 catalyst has also been synthesized to evaluate and compare its catalytic behavior. The SAPO-18 material has been prepared following the preferred

synthesis procedure described in the literature, [11] and later, the extra-framework Cu^{2+} species have been inserted by cationic exchange (see experimental for details and Table 1 for chemical compositions). This fresh Cu-exchanged SAPO-18 catalyst performs well for the SCR of NOx, achieving conversion values close to 80% for most of the tested reaction temperatures (see Figure 10a). This catalytic behavior is comparable to the one observed for CuSAPO18_5, which contains almost the same Cu content than Cu-exchanged SAPO-18 (see Table 1).

The three Cu-SAPO-18 samples synthesized by direct synthesis have been subjected to steaming treatments at 750ºC for 13 hours. The two samples synthesized with the lowest Cu contents, CuSAPO18_5 (Cu/TO_2 = 0.025) and CuSAPO18_6 (Cu/TO_2 = 0.05), preserve the original crystalline nature of the AEI structure; whereas the sample synthesized with the highest Cu content, CuSAPO18_7 (Cu/TO_2 = 0.10), undergoes a phase transformation towards a dense phase (see PXRD patterns in Figure 11). Analogous structure collapse has been described previously in the literature for similar small pore silicoaluminophosphates with high metal contents.[5b,16] This fact can be explained by the inadequate charge balance between the extra-framework metal species and the anionic zeolitic framework when large amounts of metal are present. Presumably, these catalysts will present abundant structural defects to compensate the excessive positive charges introduced by cationic metal species, resulting in unstable crystalline structures when treated under steam and high temperatures. For instance, we could assert, in a first approximation, that the much lower hydrothermal stability of CuSAPO18_7 may be explained by the presence of excessive positive charges, assuming that most of the copper species would be as Cu^{2+} (0.13 positive charges per TO_2, see Table 1), compared with the anionic framework species generated by isolated [Si(4Al)]⁻ species (0.10 negative charges, see Table 1).

The Cu-exchanged SAPO-18 catalyst has also been steamed at 750ºC for 13 hours, and as it can be observed in Figure 7, this aged catalyst has been transformed into a dense phase. In contrast, the sample CuSAPO18_5, which has been prepared by direct synthesis procedures, preserves the original crystalline nature of the AEI structure. The reason of this phase transformation could be explained by the plausible large presence of Si islands

in the synthesized silicoaluminophosphate SAPO-18 material, as broadly described in the literature.[11,12] This result clearly underlines the importance of the direct synthesis methodology to prepare efficient and stable Cu-SAPO-18 catalysts for the SCR of NOx compared to traditional Cu-exchanged SAPO-18 catalysts.

The hydrothermally stable CuSAPO18_5 and CuSAPO18_6 catalysts have also been tested for the SCR of NOx after being aged at 750ºC for 13 hours and, interestingly, both aged catalysts maintain most of their fresh catalytic activities (see Figures 10a and 10b). Indeed, the Cu-SAPO-18 catalyst containing the lowest Cu content (CuSAPO18_5, ~2.7 %wtCu) shows NO conversions of almost 80% under broad reaction temperatures for both fresh and aged catalysts (see CuSAPO18_5 and CuSAPO18_5_HT750ºC in Figures 10a and 10b, respectively), and the Cu-SAPO-18 with the intermediate Cu content (CuSAPO18_6, ~5.6 %wtCu) presents NO conversions above 90% for both fresh and aged catalysts (see CuSAPO18_6 and CuSAPO18_6_HT750ºC in Figures 10a and 10b, respectively).

The very close catalytic performances of fresh and aged counterparts would indicate that most of the extra-framework Cu^{2+} active sites would remain stable on these catalysts, even after being severely aged. To confirm this point, a preliminary characterization of the fresh and aged CuSAPO18_6 catalysts has been performed by temperature-programed reduction (TPR) with hydrogen. This technique can provide accurate information about the Cu species present in the catalysts. The only H_2 consumption peak observed for both fresh and aged CuSAPO18_6 catalysts, apperas at low temperature (~250-300ºC, see Figure 12), which has been assigned in the literature to the reduction of isolated Cu^{2+} species.[19] The absence of signals centered at 350-370ºC and 450-500ºC, associated to the reduction of bulk CuO to Cu^0 and, the reduction of Cu^+ to CuO, respectively,[19,20] demonstrates the benefits of the present direct synthesis process to preferentially insert the active cationic species of copper in the catalyst for the SCR of NOx, as well as to properly stabilize the metal cationic species against severe ageing procedures.

3.3.- Direct synthesis of Cu-SAPO-18: effect of the crystallization temperature

- *Synthesis and characterization*

The use of a specific cyclic ammonium OSDA has shown an excellent improvement of the catalytic and stability properties of the Cu-SAPO-18 catalysts for the SCR of NOx. Nevertheless, the FE-SEM image of the optimized CuSAPO18_6 material reveals an intergrowth of several cubic SAPO-18 crystals agglomerated by some bulk fine powder (see Figure 9d). Although this catalyst shows good activity and hydrothermal stability under the tested conditions, the crystallinity of the Cu-SAPO-18 catalyst should still be improved to operate under real severe conditions for very long times, in order to have industrial possibilities.

Having that in mind, we propose the direct synthesis of Cu-SAPO-18 using DMDMP as OSDA at higher temperatures to favor the nucleation and crystallization processes during the hydrothermal synthesis. Thus, two new syntheses of Cu-SAPO-18 have been attempted at 190ºC using different Cu-TETA ratios [Cu-TETA/TO_2 = 0.025, 0.05]. PXRD patterns reveal the formation of high crystalline SAPO-18 materials regardless the Cu-TETA content (see CuSAPO18_8 and CuSAPO18_9 in Figure 13), and FE-SEM images show the intergrowth of well-shaped cubic crystals of SAPO-18 with sizes ranging from 0.2 to 1 μm (see Figure 14). Although the crystal size distribution shows some heterogeneity, the overall crystallinity of these Cu-SAPO-18 samples has been notoriously increased as compared to the previous materials synthesized at 175ºC (see FE-SEM image of CuSAPO18_6 in Figure 9d).

Regarding the chemical composition, the Cu charge within these new Cu-SAPO-18 materials is also controlled depending on the initial Cu-TETA in the synthesis media, reaching values of 2.8 and 5.3 %wtCu for CuSAPO18_8 and CuSAPO18_9, respectively (see Table 1). Interestingly, these Cu amounts are comparable to the ones obtained previously for the syntheses performed at 175ºC (see CuSAPO18_5 and CuSAPO18_6 in Table 1). As it was said above, the silicon distribution along the zeolitic framework is also an important variable that will influence the activity and stability of the catalysts. Solid ^{29}Si MAS NMR on CuSAPO18_9 shows the presence of a single signal centered at -90 ppm, which has been assigned to well-distributed isolated silicon atoms, resulting in the desired materials also from the point of view of the Si distribution.

- *Catalysis and hydrothermal stability*

The hydrothermal stability of CuSAPO18_8 and _9 has been evaluated by exposing these catalysts to steam at 750ºC for 13 hours. As their PXRD patterns reveal, these two materials preserve their original crystalline structure after being steamed (see Figure 13) and, most importantly, the catalytic activity for the SCR of NOx of the two steamed Cu-SAPO-18 catalysts is higher than 90% for most of the tested reaction temperatures (see Figure 15). Particularly interesting is the catalytic activity achieved for the steamed CuSAPO18_9 catalyst, which proceeds with NO conversion values of almost 100% for most of the studied temperatures (see Figure 15).

Other well-known related efficient catalysts for the SCR of NOx have been introduced to compare their catalytic activity with the hydrothermally stable Cu-SAPO-18 materials. On one hand, the Cu-exchanged silicoaluminate form of the AEI structure, Cu-SSZ-39 zeolite, that has been recently reported as very efficient catalyst for the SCR of NOx;[9] and on the other hand, the optimized form of the Cu-SAPO-34 material prepared following similar "one-pot" synthesis methodologies.[16] As it can be seen in Figure 15, steamed Cu-SAPO-18 at 750ºC for 13 hours performs similarly to the optimized Cu-SAPO-34 and Cu-SSZ-39 when tested under very harsh reaction conditions (high space velocity and presence of water in the feed), revealing the outstanding catalytic behavior of the Cu-SAPO-18 catalyst.

Preliminary characterization of the calcined and steamed CuSAPO18_9 using temperature-programed reduction (TPR) with hydrogen, indicate that the main H_2 consumption peak for both fresh and aged CuSAPO18_9 catalysts is centered at ~250-300ºC, which has been assigned in the literature to the reduction of isolated Cu^{2+} species (see Figure 12).[19] The results indicate that most of the copper species are as extra-framework Cu^{2+} cations, even after severe ageing procedures. This result points out the very high hydrothermal stability of these Cu-SAPO-18 catalysts synthesized by a "one-pot" procedure.

4.- Conclusions

16

The combination of an organometallic Cu-complex, as Cu^{2+} with triethylenetetramine (Cu-TETA), and N,N-dimethyl-3,5-dimethylpiperidinium (DMDMP) as OSDAs has allowed the direct preparation of very active and hydrothermally stable Cu-SAPO-18 catalysts for the selective catalytic reduction (SCR) of NOx. Different characterization techniques suggest that the copper species are mainly as extra-framework Cu^{2+}, which have been described as the specific active sites for the SCR of NOx, and very interestingly, the selective presence of isolated Si species in the zeolitic framework introduces high hydrothermal stabilities to these Cu-SAPO-18 catalysts.

Acknowledgments

Figure 1: Synthesis conditions studied using N,N-diisopropylethylamine (DIPEA) as OSDA combined with two different Cu-complexes (Cu-TETA and Cu-TEPA). Hydrothermal syntheses are carried out at T=175ºC for 12 h under static conditions.

	P/Al=0.85 Si/(Al+P) = 0.081		P/Al=0.9 Si/(Al+P) = 0.053	
	Cu-TEPA/(Al+P)		Cu-TEPA/(Al+P)	
	0.025	0.05	0.025	0.05
H$_2$O/(Al+P) = 5	CuSAPO18_1	(SAPO-18 + SAPO-34)	CuSAPO18_2	(SAPO-18 + Dense Phase)
	Cu-TETA/(Al+P)		Cu-TETA/(Al+P)	
	0.025	0.05	0.025	0.05
H$_2$O/(Al+P) = 5	CuSAPO18_3	CuSAPO18_4	(SAPO-18)	(SAPO-18 + Dense Phase)

SAPO-18
SAPO-18 + Dense Phase
SAPO-18 + SAPO-34

Figure 2: PXRD patterns of Cu-SAPO-18 materials synthesized using N,N-diisopropylethylamine (DIPEA) as OSDA combined with different Cu-complexes.
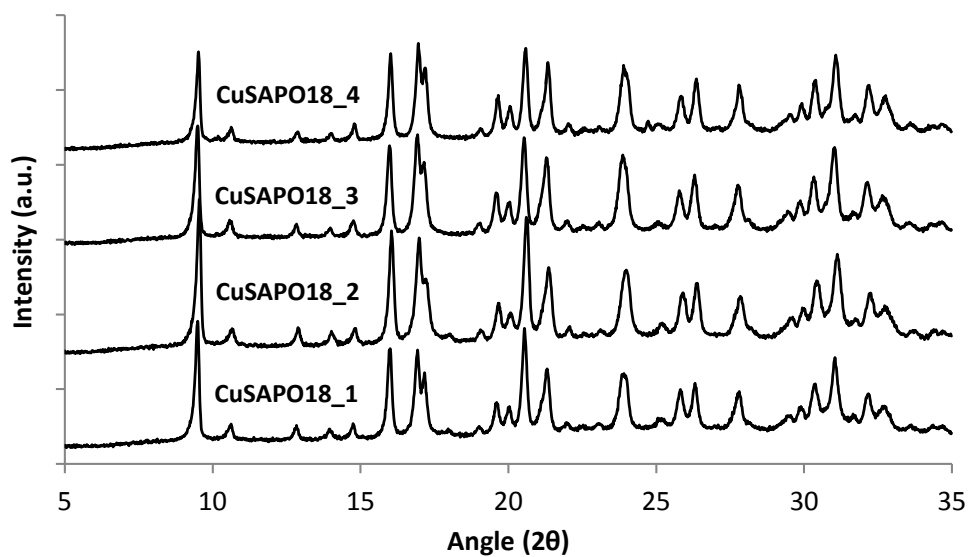
Figure 3: UV-VIS spectra of the as-prepared CuSAPO18_1 and Cu-TEPA complex in solution.
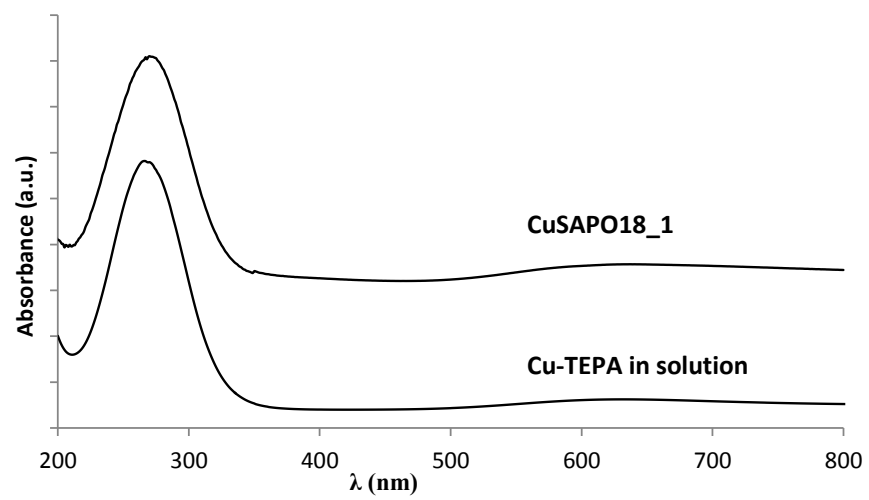
Figure 4: ^{29} Si MAS NMR spectra of different Cu-SAPO-18 materials.
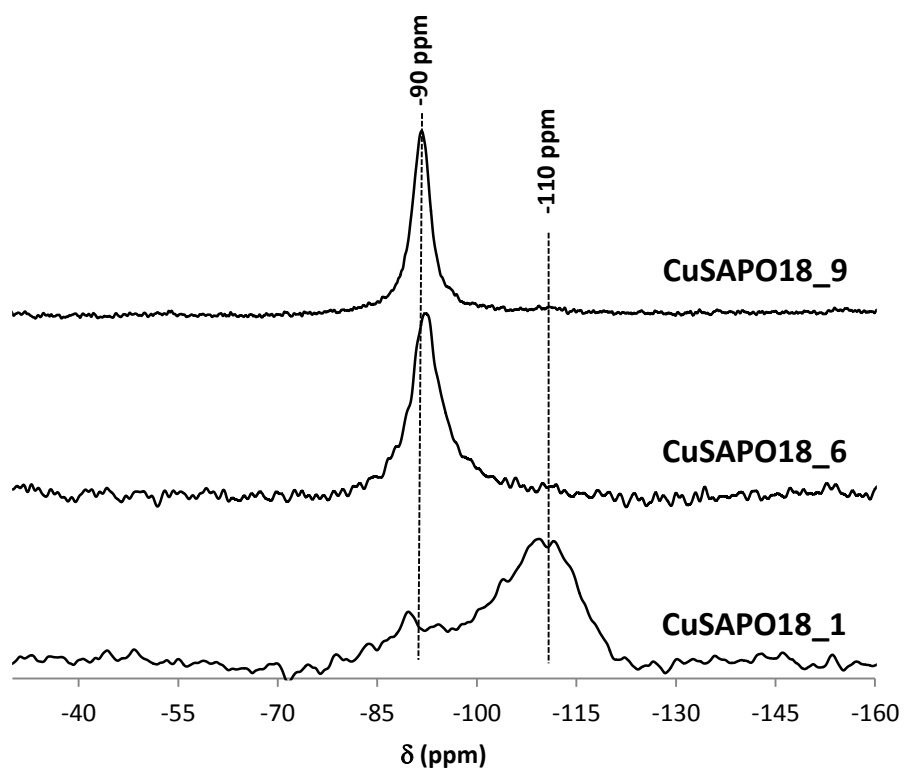
Figure 5: Catalytic activity for the SCR of NOx of Cu-SAPO-18 materials synthesized using N,N-diisopropylethylamine as OSDA.
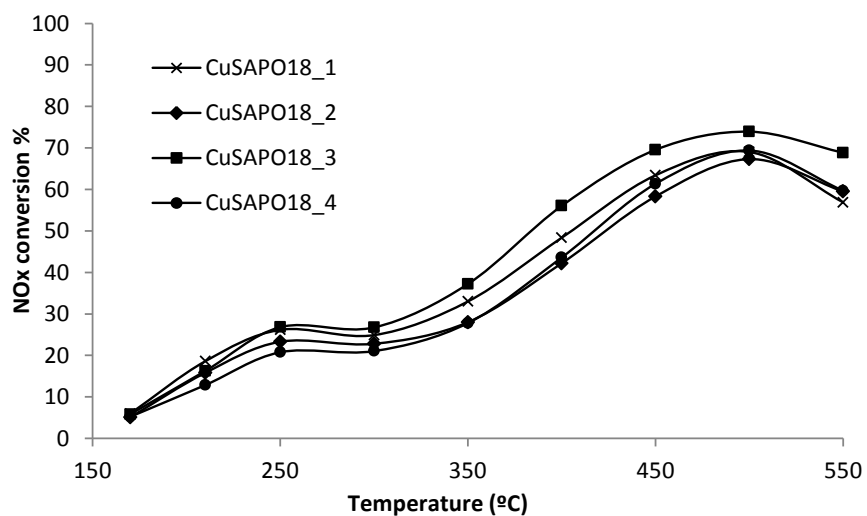
Figure 6: Synthesis conditions studied using DMDMP as OSDA combined with Cu-TETA. Hydrothermal syntheses are carried out at T=175ºC for 6 d under dynamic conditions.

	P/Al = 0.85		
	Si/(Al+P) = 0.081		
	Cu-TETA/(Al+P)		
	0.025	0.05	0.1
DMDMP/(Al+P)	0.475	0.45	0.4
H₂O/(Al+P) 10			
H₂O/(Al+P) 30	CuSAPO18_5	CuSAPO18_6	CuSAPO18_7

▮	SAPO-18
☰	SAPO-18 + Dense Phase

Figure 7: PXRD patterns of Cu-SAPO-18 materials synthesized using DMDMP as OSDA combined with Cu-TETA at 175ºC, and Cu-exchanged SAPO-18 using DIPEA as OSDA.
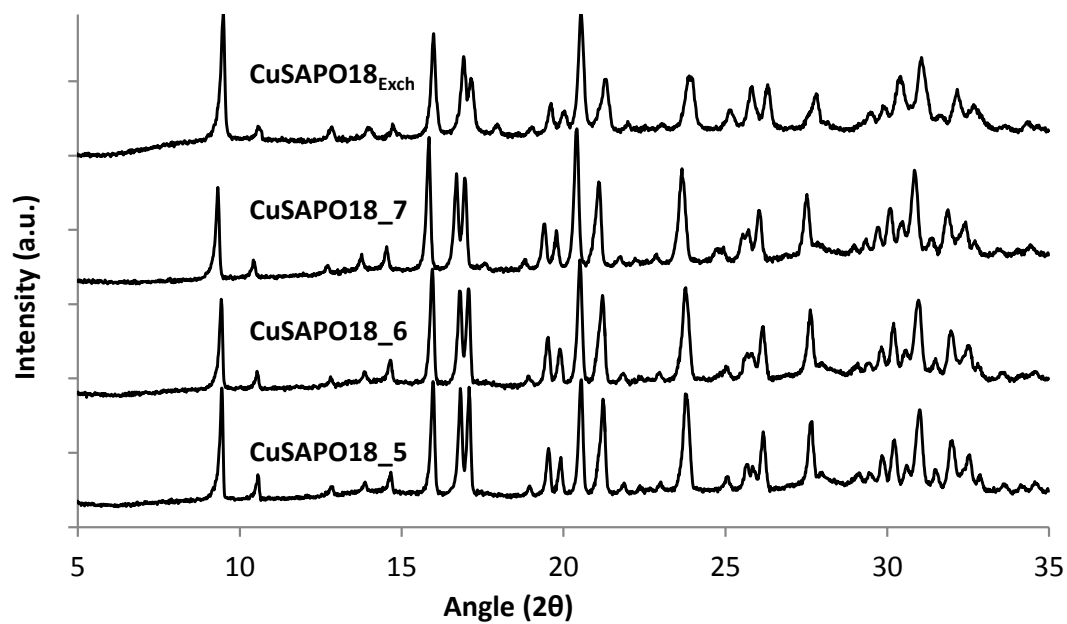
Figure 8: UV-VIS spectra of the as-prepared CuSAPO18_6 and Cu-TETA complex in solution.
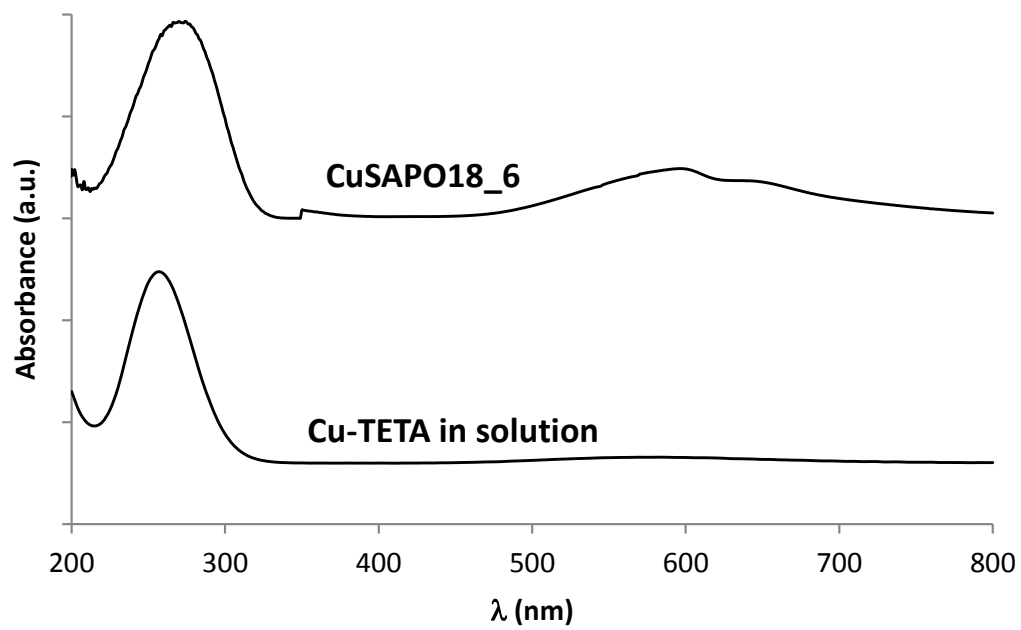
Figure 9: SEM images of CuSAPO18_5 (A), CuSAPO18_6 (B) and CuSAPO18_7 (C), and FE-SEM image of CuSAPO18_6 (D).
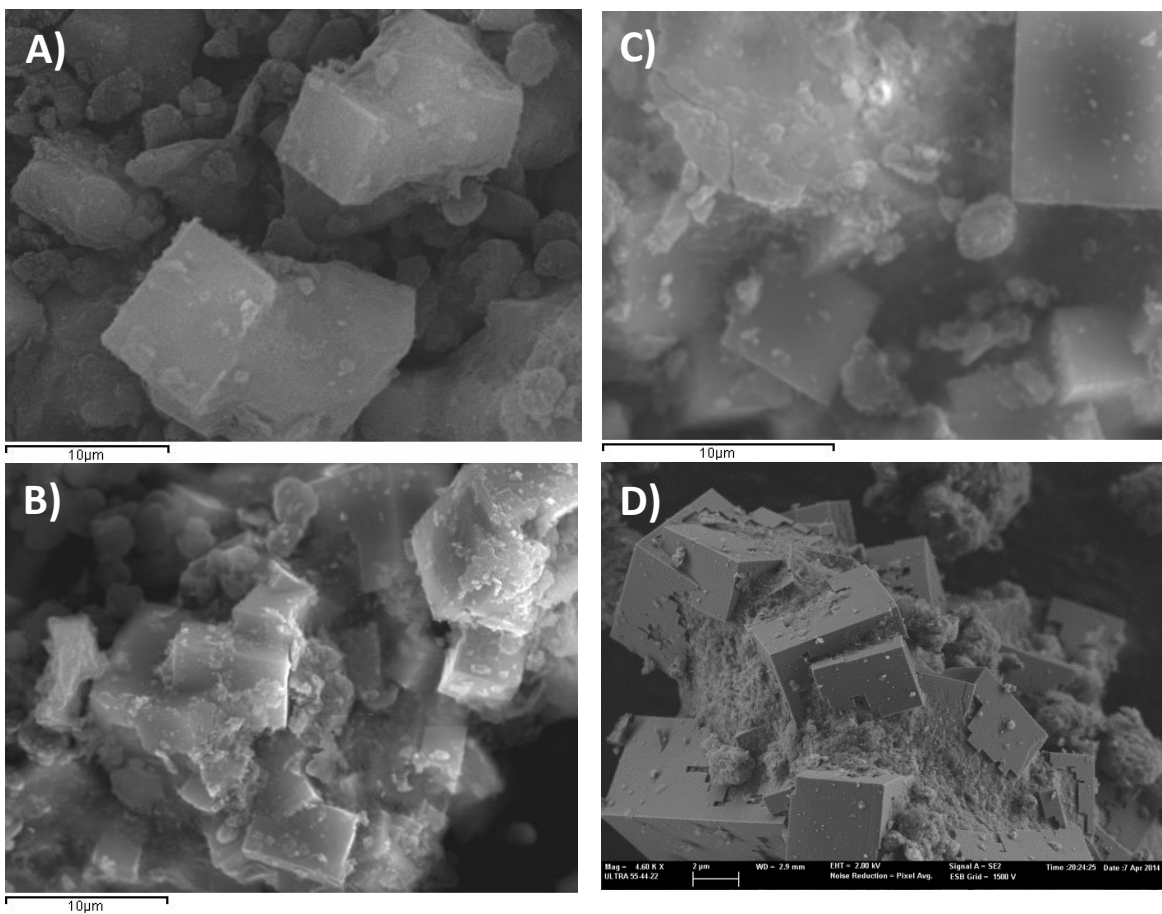
Figure 10: Catalytic activity for the SCR of NOx reaction of Cu-SAPO-18 materials synthesized at 175ºC using DMDMP after calcination at 550ºC and Cu-exchanged SAPO-18 (A) and after steam treatment at 750ºC for 13 h (B).
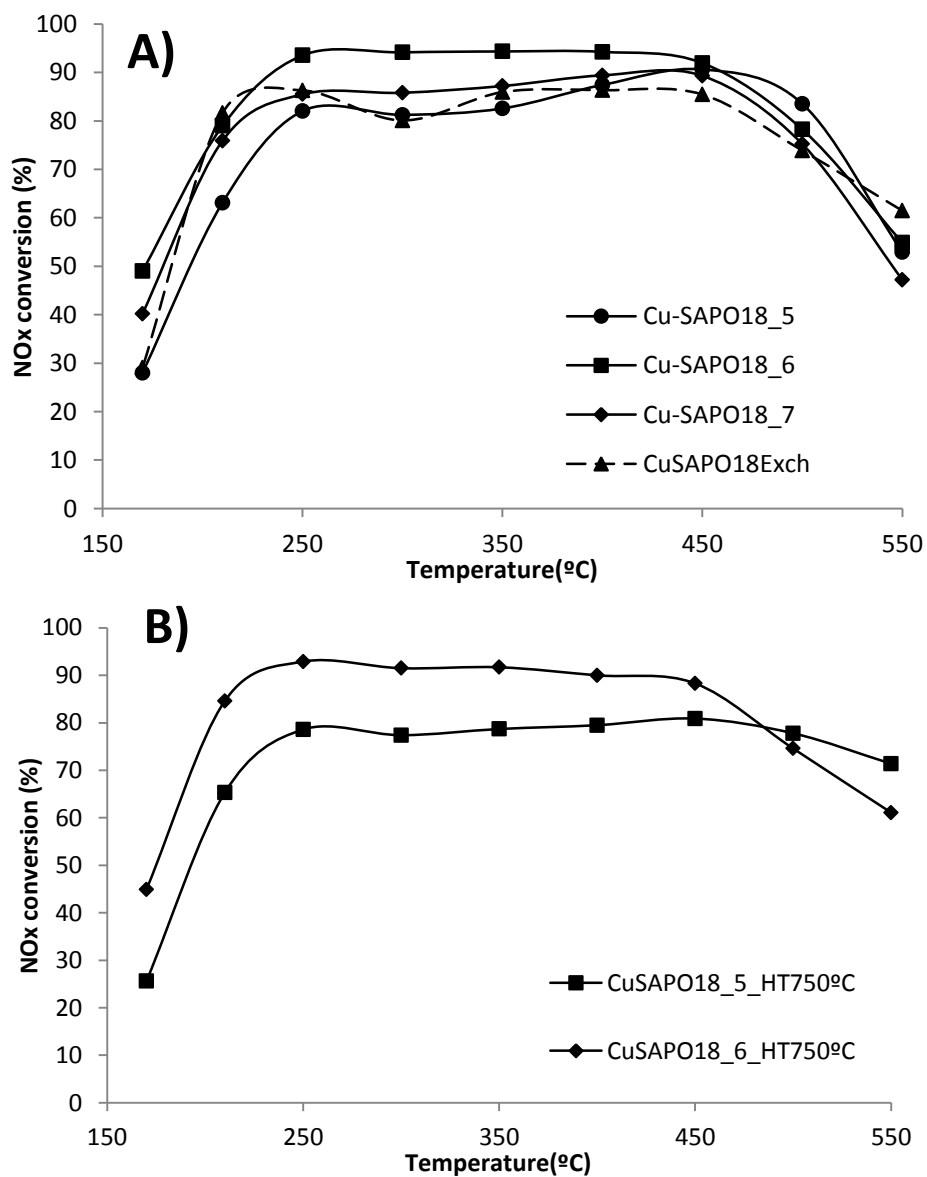
Figure 11: PXRD after steaming at 750ºC for 13 hours patterns of Cu-SAPO-18 materials synthesized using DMDMP at 175ºC, and Cu-exchanged SAPO-18 synthesized using DIPEA.
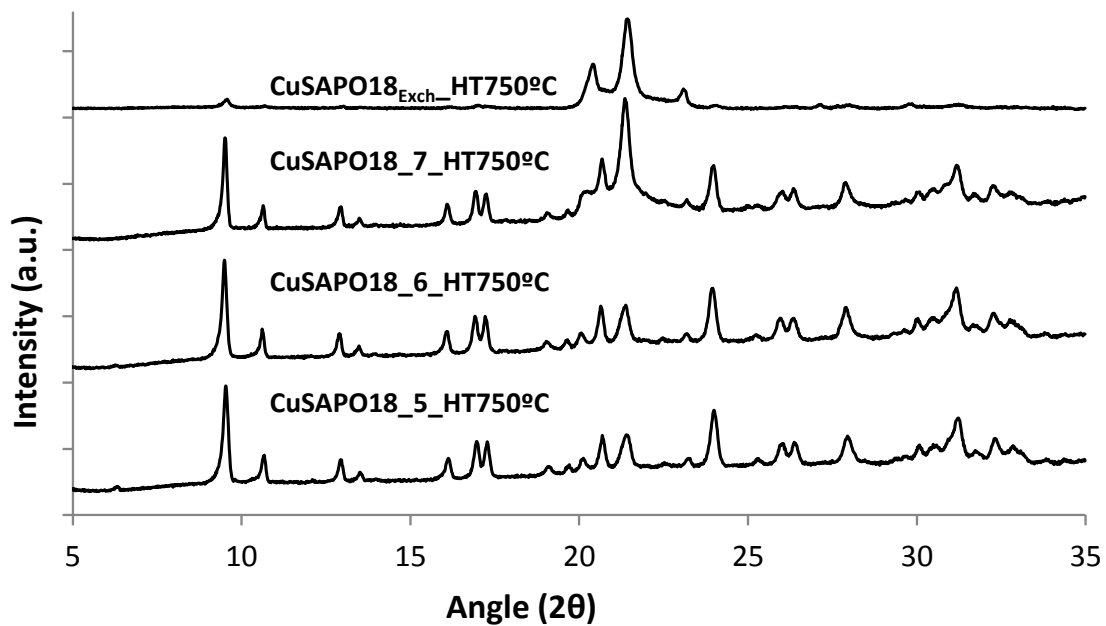
Figure 12: H$_2$-TPR profile of calcined and steamed at 750ºC CuSAPO18_6 and CuSAPO18_9 catalysts
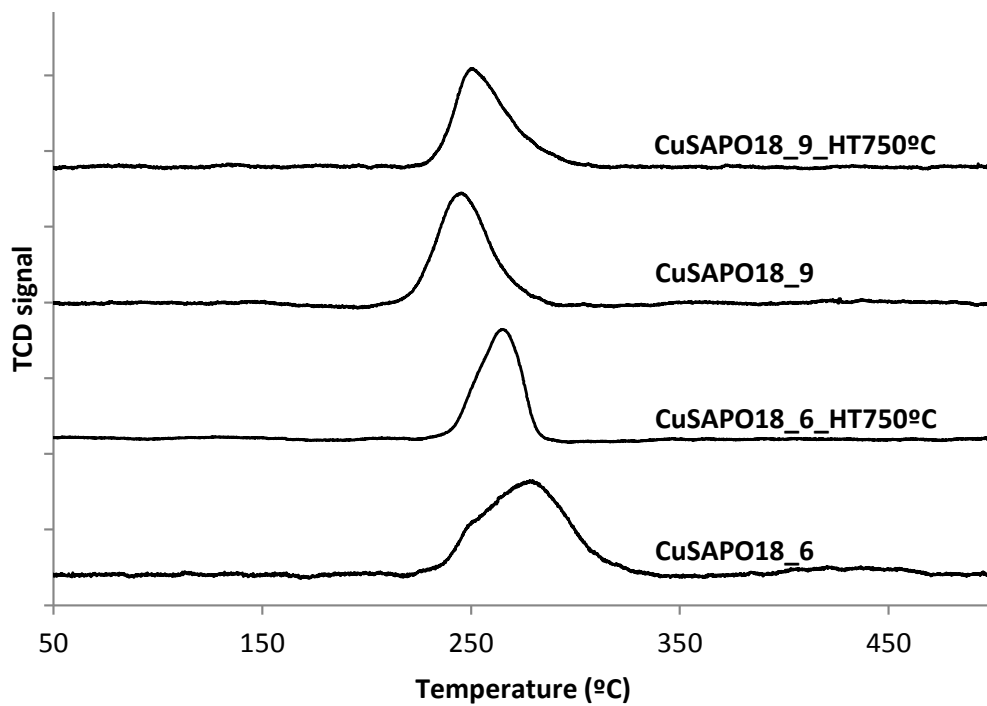
Figure 13: PXRD patterns of the as-prepared and steamed Cu-SAPO-18 materials synthesized using N,N-dimethyl-3,5-dimethylpiperidinium (DMDMP) as OSDA combined with Cu-TETA at 190ºC.
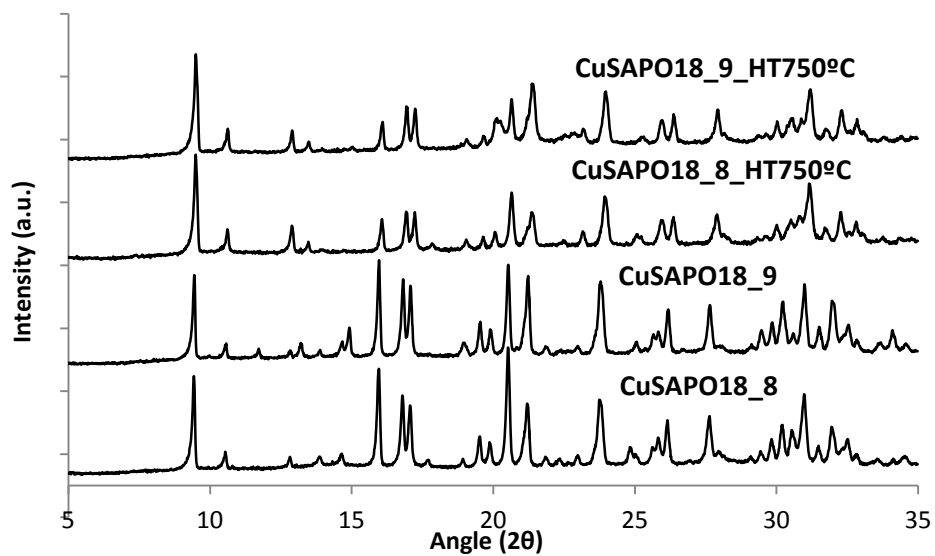
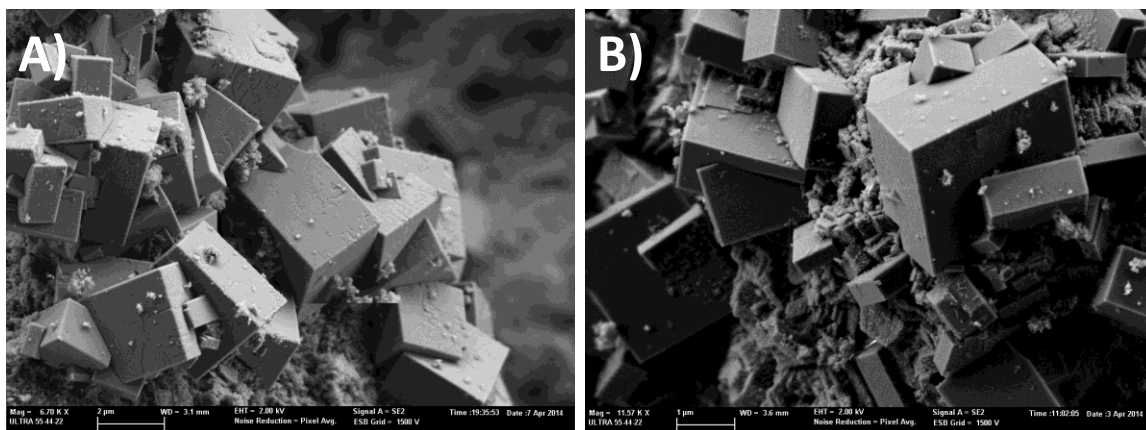**Figure 14: FE-SEM images of CuSAPO18_8 (A) and CuSAPO18_9 (B).**

Figure 15: Catalytic activity for the SCR of NOx reaction of Cu-SAPO-18 materials synthesized at 190ºC using DMDMP and different amount of Cu-TETA after steaming at 750ºC for 13 h.
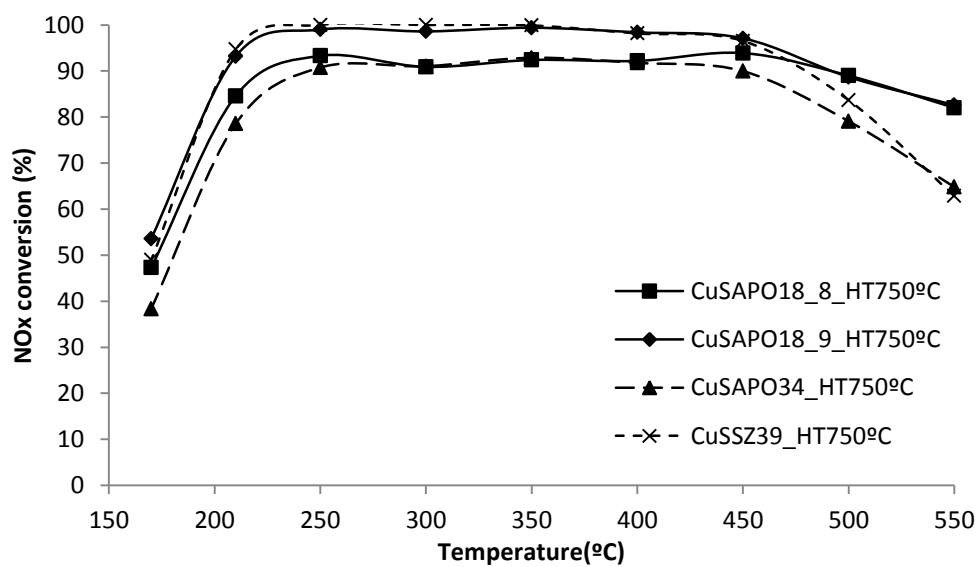
Table 1: Chemical and elemental analyses of Cu-SAPO-18 materials

Sample	Si/(Al+P)	Cu/(Al+P)	wt%Cu	TETA/(Al+P)	Solid yield (%wt)
CuSAPO18_1	0.120	0.029	2.6	---	90-95
CuSAPO18_5	0.097	0.028	2.7	---	90-95
CuSAPO18_6	0.101	0.056	5.6	0.063	90-95
CuSAPO18_7	0.104	0.065	6.2	---	85-90
CuSAPO18_8	0.089	0.029	2.8	---	85-90
CuSAPO18_9	0.090	0.055	5.3	0.055	90-95
CuSAPO18$_{Exc}$	0.067	0.023	2.5	---	---

References:

[1] M. Moliner, C. Martínez, A. Corma, *Chem. Mater.*, **2014**, *26*, 246.

[2] I. Bull, R. S. Boorse, W. M. Jaglowski, G. S. Koermer, A. Moini, J.A. Patchett, W. M. Xue, P. Burk, J. C. Dettling, M. T. Caudle, *U.S. Patent 0,226,545*, **2008**.

[3] a) S. Brandenberger, O. Kröcher, A. Tissler, R. Althoff, *Catal. Rev. Sci. Eng.*, **2008**, *50*, 492; b) M. W. Twigg, *Appl. Catal. B*, **2007**, *70*, 2.

[4] a) J. H. Kwak, R. G. Tonkyn, D. H. Kim, J. Szanyi and C. H. F. Peden, *J. Catal.*, **2010**, *275*, 187; b) S. T. Korhonen, D. W. Fickel, R. F. Lobo, B. M. Weckhuysen and A. M. Beale, *Chem. Commun.*, **2011**, *47*, 800.

[5] a) I. Bull, U. Muller, *US2010/0310440A1*, **2010**; b) R. Martínez-Franco, M. Moliner, C. Franch, A. Kustov, A. Corma, *Appl. Catal. B* **2012**, *127*, 273; c) U. Deka, I. Lezcano-Gonzalez, S. J. Warrender, A. L. Picone, P. A. Wright, B. M. Weckhuysen, A. M. Beale, *Micropor. Mesopor. Mater.* **2013**, *166*, 144; d) L. Ma, Y. Cheng, G. Cavataio, R. W. McCabe, L. Fu, J. Li, *Chem. Eng. J.*, **2013**, *225*, 323; e) P. N. R. Vennestrøm, A. Katerinopoulou, R. R. Tiruvalam, A. Kustov, P. G. Moses, P. Concepcion, A. Corma, *ACS Catal.*, **2013**, *3*, 2158.

[6] a) M. Iwamoto, H. Furukawa, Y. Mine, F. Uemura, S.I. Mikuriya, S. Kagawa, *J. Chem. Soc., Chem. Commun.*, **1986**, 1272; b) B. Modén, P. Da Costa, B. Fonfé, D. K. Lee, E. Iglesia, *J. Catal.*, **2002**, *209*, 75; c) M. H. Groothaert, J. A. van Bokhoven, A. A. Battiston, B. M. Weckhuysen, R. A. Schoonhetdt, *J. Am. Chem. Soc.*, **2003**, *125*, 7629; d) A. Corma, V. Fornés, A. E. Palomares, *Appl. Catal. B*, **1997**, *11*, 233.

[7] a) D. W. Fickel, R. F. Lobo, *J. Phys. Chem. C*, **2010**, *114*, 1633; b) S. A. Bates, A. A. Verma, C. Paolucci, A. A. Parekh, T. Anggara, A. Yezerets, W. F. Schneider, J. T. Miller, W. N. Delgass, F. H. Ribeiro, *J. Catal.*, **2014**, *312*, 87.

[8] D. W. Fickel, E. D'addio, J. A. Lauterbach, R. F. Lobo, *Appl. Catal. B*, **2011**, *102*, 441.

[9] M. Moliner, C. Franch, E. Palomares, M. Grill, A. Corma, *Chem.Commun.*, **2012**, *48*, 8264.

[10] a) S. I. Zones, Y. Nakagawa, S. T. Evans and G. S. Lee, U.S. Patent, 5,958,370, 1999; b) P. Wagner, Y. Nakagawa, G. S. Lee, M. E. Davis, S. Elomari, R. C. Medrud, S. I. Zones, *J. Am. Chem. Soc.*, **2000**, *122*, 263.

[11] J. Chen, P. A. Wright, J. M. Thomas, S. Natarajan, L. Marchese, M. Bradley, G. Sankar, C. R. A. Catlow, *J.Phys. Chem.*, **1994**, *98*, 10216.

[12] a) J. Chen, J. M. Thomas, P. A. Wright, Catal. Lett., 1994, 28, 241; b) M. Hunger, M. Seiler, A. Buchholz, *Catal. Lett.*, **2011**, *74*, 61; c) D. Fan, P. Tian, S. Xu, Q. Xia, X. Su, L. Zhang, Y. Zhang, Y. He, Z. Liu, *J. Mater. Chem.*, **2012**, *22*, 6568.

[13] a) A. G. Gayubo, A. T. Aguayo, A. Alonso, A. Atutxa, J. Bilbao, *Catal. Today*, **2005**, *106*, 112; b) A. G. Gayubo, A. T. Aguayo, A. Alonso, J. Bilbao, *Ind. Eng. Chem. Res.*, **2007**, *46*, 1981; c) M. M. Mertens, *U.S. Patent 20090238745*, **2009**; d) W. Vermeiren, N. Nesterenko, *Eur. Pat. Appl. 2027918*, **2009**; e) D. S. Wragg, D. Akporiaye, H. Fjellvag, *J. Catal.*, **2011**, *279*, 397; (f) J. Chen, J. Li, Y. Wei, C. Yuan, B. Li, S. Xu, Y. Zhou, J. Wang, M. Zhang, Z. Liu, *Catal. Commun.*, **2014**, *46*, 36.

[14] a) Q. Ye, L. Wang, R. T. Yang, *Appl. Catal. A*, **2012**, *427-428*, 24; b) Q. Ye, H. Wang, S. Cheng, D. Wang, T. Kang, *CN 102626653*, **2012**.

[15] R. Vomscheid, M. Briend, M. J. Peltre, P. P. Man, D. Barthomeu, *J. Phys.Chem.* **1994**, *98*, 9614.

[16] R. Martínez-Franco, M. Moliner, P. Concepción, J. R. Thogersen, A. Corma, *J. Catal.*, **2014**, *314*, 73.

[17] a) L. Ren, L. Zhu, C. Yang, Y. Chen, Q. Sun, H. Zhang, C. Li, F. Nawaz, X. Meng, F. S. Xiao, *Chem. Commun.*, **2011**, *47*, 9789; b) R. Martinez-Franco, M. Moliner, J. R. Thogersen, A. Corma, *ChemCatChem*, **2013**, *5*, 3316; c) U. Deka, I. Lezcano-Gonzalez, S. J. Warrender, A. L. Picone, P. A. Wright, B. M. Weckhuysen, A. M. Beale, *Micropor. Mesopor. Mater*. **2013**, *166*, 144.

[18] R. Martinez-Franco, M. Moliner-Marin, A. Corma-Canos, A. Kustov, J. R. Thoegersen, J. *WO 2013159828*, **2013**.

[19] a) Y. Wan, J. Ma, Z. Wang, W. Zhou, S. Kaliaguine, *J. Catal*. **2004**, *227*, 242; b) A. Sultana, T. Nanba, M. Haeda, M. Sasaki, H. Hamada, *Appl. Catal. B*. **2010**, *101*, 61.

[20] M. Richter, M. J. G. Fait, R. Eckelt, *Appl. Catal. B*. **2007**, *73*, 269.